Optimization of the dimensional stability of paper-based sandwich panels during the pressing process using design of experiments

Yuting Wei[1], **Franz Hirsch**[1], **Dietmar Süße**[1], **Birgit Lutsch**[2], and **Markus Kästner**[1]*

[1] Institute of Solid Mechanics, TU Dresden, 01062 Dresden, Germany
[2] Papiertechnische Stiftung, 01809 Heidenau, Germany

In this contribution, the causes leading to the undesired unevenness on the exterior surface of a paper-based sandwich structure during the manufacturing process are investigated. This provides insight into the manufacturing parameters that need to be adjusted to reduce this waviness. A finite element model of the pressing process is developed in the commercial software *ABAQUS* and then used to analyze the formation of the surface unevenness. The sandwich structure adopted in the model consists of a decorative layer, an intermediate layer, a corrugated core and a bottom layer. In particular, the core has a sinusoidal structure with various geometry parameters, which are adjusted in the model to investigate the effect on the waviness of the top surface. The results of the quasi-static process simulation correlate well with the experimental results. A subsequent parameter study based on the design of experiments (DoE) shows the relationship between the material parameters of the intermediate/bottom layer and the resulting waviness.

1 Introduction

The demand for lightweight construction in the automotive industry has risen significantly in recent years to attain economic and energy sustainability. Paper-based sandwich structures with a corrugated core can achieve these needs. In these conventional sandwich panels, where the intermediate layer consists of glass fibers and a polyurethane matrix (PU matrix) [1]. In contrast, this study investigates natural paper-based sandwich composites that improve the recyclability of automotive components. However, there are still limitations due to the formation of undesired waviness structures on exterior surfaces and a lack of dimensional accuracy during the manufacturing process, which includes pressing steps necessary to join the intermediate/bottom layer and the core [2–4].

2 Modeling approach

The objective is to provide a finite element model to explore the relationship between the manufacturing process and the resultant shape deviations. The structure of the investigated sandwich panel is depicted in Fig. 1 with a corrugated core in the middle, the adjacent bottom and intermediate layer, and a decorative layer [2]. The composite layers have different thicknesses, while their lengths and widths maintain the same dimensions. The intermediate and the bottom layer of this panel have identical material parameters.

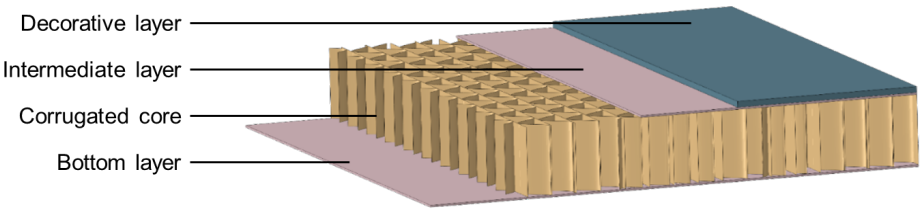

Fig. 1: Sandwich panel structure [2]

The sinusoidal core consists of liners and flutes, as shown in Fig. 2. It is characterized by small cell widths and higher compressive strength [5]. The function

$$y_i = h_{\text{flute}} \cdot \sin(\frac{2\pi}{P} \cdot (x - x_{i0})) \tag{1}$$

is used for the geometric definition of the flutes, with h_{flute}=2.5 mm, P=10 mm and a random shift x_{i0}, where i is the serial number of the flutes. The continuous automatic cutting technique causes the initial shift of sinusoidal flutes to be random [5]. Therefore, the shift of the function is chosen arbitrarily to achieve a reasonable approximation to reality.

* Corresponding author: markus.kaestner@tu-dresden.de

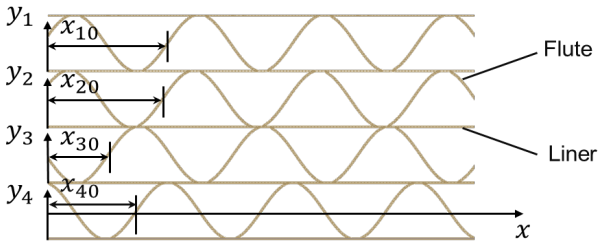

Fig. 2: Geometry and structure of the sinusoidal core

The panel is manufactured in a hot pressing process, which is numerically analyzed in two separate steps. In the first step the influence of thermal expansion is investigated, which is negligible compared to the pressing process in the second step. Hence, the hot pressing process is simplified as a single isothermal pressing process. During this process, the upper mold is moved vertically at a speed of 0.5 mm/s until the set pressing distance u, see Fig. 3.

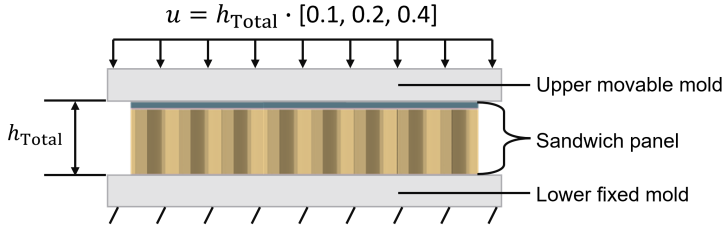

Fig. 3: Simulation setup: The pressing distance u is related to h_{Total} [2].

Since the thickness of all layers in this structure is significantly smaller than the other dimensions, shell elements are used. The corrugated core is discretized with conventional shell elements (S4R), whereas all the remaining layers are discretized with continuum shell element (SC8R), as their thickness variations during the process should not be neglected. The molds are as rigid bodies since they are far stiffer than the panel.

2.1 Identification of material parameters

In this study, tensile tests were performed for all materials involved in the panel.The decorative layer is made of a thermoplastic material and the core of corrugated paper, neither of which was altered during the study. In contrast, the properties of the interlayer are varied to study its influence. Therefore, the paper materials T1, P15, MB, and EC for the intermediate layer are investigated.

The machine-manufactured paper described as orthotropic elastic-plastic material and defined by the three principal material directions in machine direction (MD), cross direction (CD) and through-thickness direction (ZD), see Fig. 4.

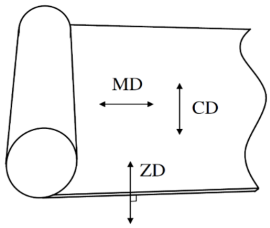

Fig. 4: Principal directions of paper

Table 1: Experimentally determined material parameters for the intermediate layer

Material	E_{MD} /MPa	E_{CD} /MPa	$\nu_{\mathrm{MD\_CD}}$/-	t /mm
T1	5181	2622	0.37	0.42
P15	2416	1112	0.37	0.76
MB	2877	1630	0.68	0.45
EC	5832	2616	0.47	0.43

Table. 1 lists all experimentally determined elastic parameters in MD and CD direction, and the thickness t of studied intermediate layer materials. The properties in ZD are difficult to determine experimentally. Therefore, the missing parameters are estimated by

$$E_{\mathrm{ZD}} = \frac{E_{\mathrm{MD}}}{200}, \quad G_{\mathrm{MD-CD}} = 0.378\sqrt{E_{\mathrm{MD}} \cdot E_{\mathrm{CD}}}, \quad G_{\mathrm{MD-ZD}} = \frac{E_{\mathrm{MD}}}{55}, \quad G_{\mathrm{CD-ZD}} = \frac{E_{\mathrm{MD}}}{35}, \tag{2}$$

where E_{MD}, E_{CD} and E_{ZD} are Young's moduli according to the principal directions of the paper, and $G_{\mathrm{MD-CD}}$, $G_{\mathrm{MD-ZD}}$ and $G_{\mathrm{CD-ZD}}$ are shear moduli [6–8]. The Poisson's ratios $\nu_{\mathrm{MD-ZD}}$ and $\nu_{\mathrm{CD-ZD}}$ are assigned a small value of 0.01 because the paper material is assumed to be stressed with plane stress conditions [9].

The plastic part of the orthotropic material uses the Hill criterion $\bar{\sigma}_{\mathrm{hill}} - \sigma_{\mathrm{y}} \leq 0$, in which the Hill potential function $\bar{\sigma}_{\mathrm{hill}}$ can be represented as a rectangular Cartesian stress component as

$$\bar{\sigma}_{\mathrm{hill}} = \sqrt{F(\sigma_{22} - \sigma_{33})^2 + G(\sigma_{33} - \sigma_{11})^2 + H(\sigma_{11} - \sigma_{22})^2 + 2L{\sigma_{23}}^2 + 2M{\sigma_{31}}^2 + 2N{\sigma_{12}}^2}, \tag{3}$$

where F, G, H, L, M, and N are constants obtained by tests of the material in different orientations [11]. The material begins to yield when the calculated stress $\bar{\sigma}_{\mathrm{hill}}$ reaches the yield stress σ_{y} on the yield surface.

2.2 Analysis of surface waviness

Surface waviness is examined on the manufactured and simulated parts. The 3D Optical Profilometer VR 3200 by Keyence was used to capture the entire surface of the real part and evaluate the waviness values, see in Fig. 5.

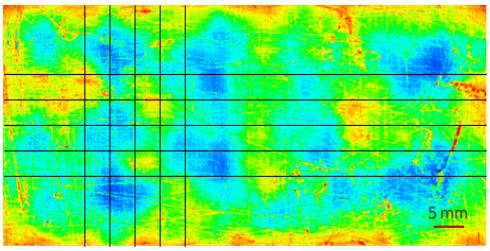

Fig. 5: Determination of five 1D height profiles in each direction

In addition, the height profile of the surfaces was extracted from the simulation results and then assessed using a Gaussian filter. The Gaussian filter is applied to limit the wavelength of the data, meaning both waviness above the long and below the short wavelengths are not studied. This study aims at investigating waviness W_a with waviness lengths between 0.8 mm and 8 mm using the arithmetic means

$$W_a = \frac{1}{l} \int_l^0 |z(x)|\, dx, \tag{4}$$

which is shown in Fig.6.

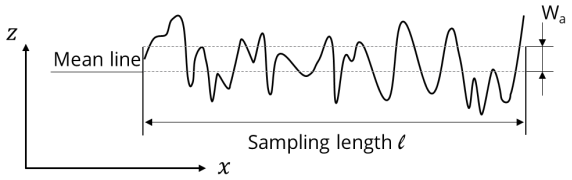

Fig. 6: Calculation of the waviness value W_a

3 Results

The numerical process model is validated by comparison of the experimental and simulation results in this section. Afterward, the relationship between the properties of the intermediate/bottom layer and the surface waviness W_a is analyzed using DoE.

3.1 Validation of the process modeling approach

Several simulations were performed with the numerical process model and the previously presented material properties. The shape of corrugated cores can not ensure to remain identical because the flutes and liners of the core are randomly bonded, see Fig. 2. Hence, an important fact that must be made clear is that the same results from experiments and simulations are not expected when the effect of the initial phase shift on the waviness can not be excluded [12].

Waviness values W_a from the experimental and simulation results are shown in Fig 7(a)-(d) for different u and different materials for the intermediate layer corresponding to Tab. 1. The presented results indicate that u and different materials for the intermediate layer have no significant association with the observed W_a. Nevertheless, the experimental and simulation results are in the same order of magnitude, and their differences are within acceptable limits.

Moreover, the experimental results with the same conditions may differ considerably, for example for the paper EC with a pressing distance $u = 0.4 \cdot h_{\mathrm{Total}}$, see Fig. 7(d). It can be noticed that the initial phase shift x_{i0} of the sinusoidal core in Fig. 2 was kept constant in the simulations. In contrast, each manufactured panel exhibits a random shift. This influence is

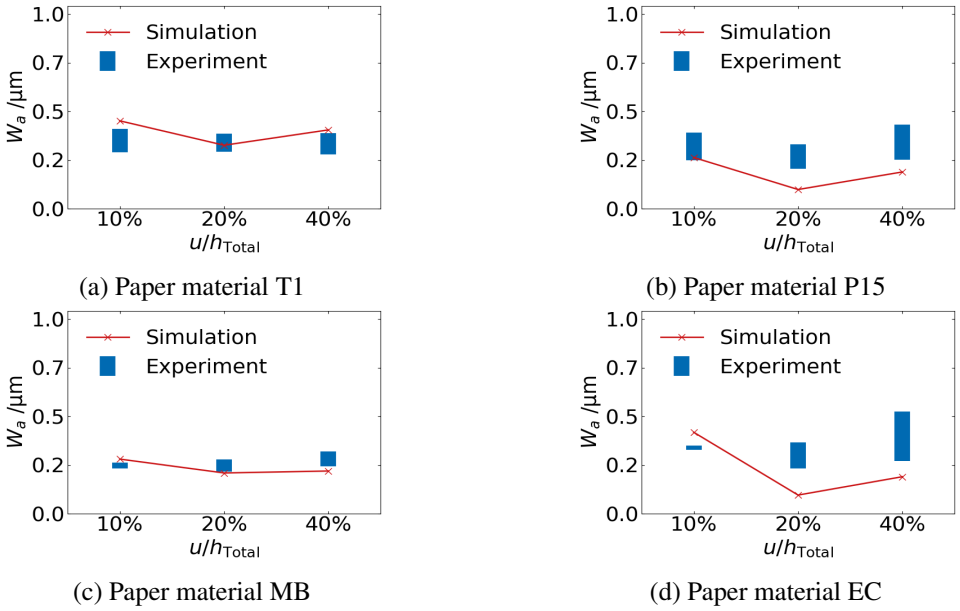

(a) Paper material T1 (b) Paper material P15

(c) Paper material MB (d) Paper material EC

Fig. 7: Comparison of waviness W_a from experimental and simulation results for different u and intermediate layers

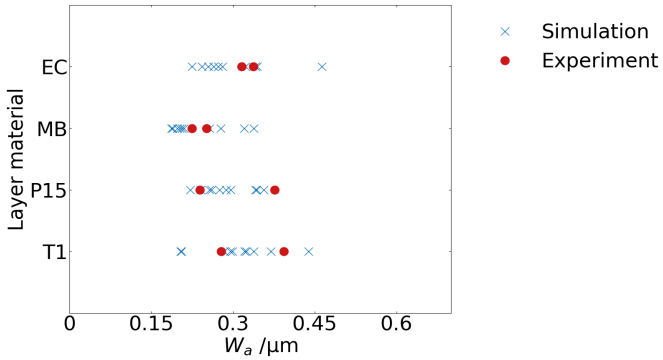

Fig. 8: Results of the experiments and the simulations using random initial phase shifts

investigated in the following. Simulations with 24 random sets of initial phase shift x_{i0} for each material combination were performed, see Fig. 8.

Figure 8 decipts results of the experiments and the simulations using random initial phase shifts x_{i0} with pressing distance u=0.1·h_{Total}. The blue cross symbols and red dots respond to the simulation and the experimental results, respectively. The experimental results are all within the range of the simulation results, indicating that x_{i0} significantly affects the results. Furthermore, the paper MB performs best with the smallest W_a in experiments and simulations, which reveals that the material properties of the intermediate layer influence the surface waviness during the manufacturing process. However, the geometry of the corrugated core can also lead to considerably different waviness values.

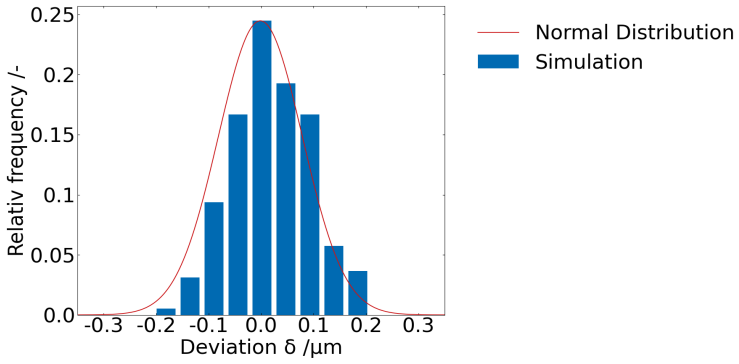

Fig. 9: The deviation δ obeys the normal distribution

The deviation between simulation and experiment is defined by

$$\delta = |u_{\text{sim}} - \bar{u}_{\text{exp}}|\,, \tag{5}$$

where u_{sim} is the simulation result, and $\bar{u}_{\text{exp}}$ is the mean value of the experimental results. The deviations δ based on Fig. 8 are divided into ten groups, and their relative frequencies are shown in Fig. 9, which obey a normal distribution since x_{i0} was created with a random generator. Hence, the numerical model is verified by comparing the experimental and simulation results.

3.2 Investigation of the causes of waviness

DoE is a method for determining the correlation between input and target variables. This method is used to identify the most critical parameter of the intermediate layer on W_a since x_{i0} is an uncontrollable variable in the experiment. Parameters of interest are the mechanical properties and the layer thickness.

Figure 10 shows the 30 combinations of the layer thickness t and Young's in MD, which are investigated in this study.

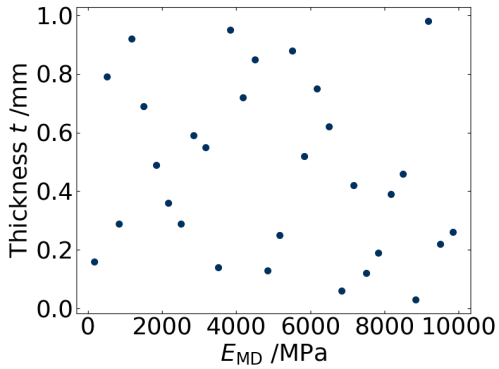

Fig. 10: Parameter combinations for the intermediate/bottom layer using DoE

Based on the parameters of typical paper materials, the thickness t range was designated from 0.03 to 1 mm, and E_{MD} was varied from 181 to 10,000 MPa. All other mechanical properties in Tab. 1 and Equ. 2 are based on the proportional relationship between the mechanical properties of the paper T1.

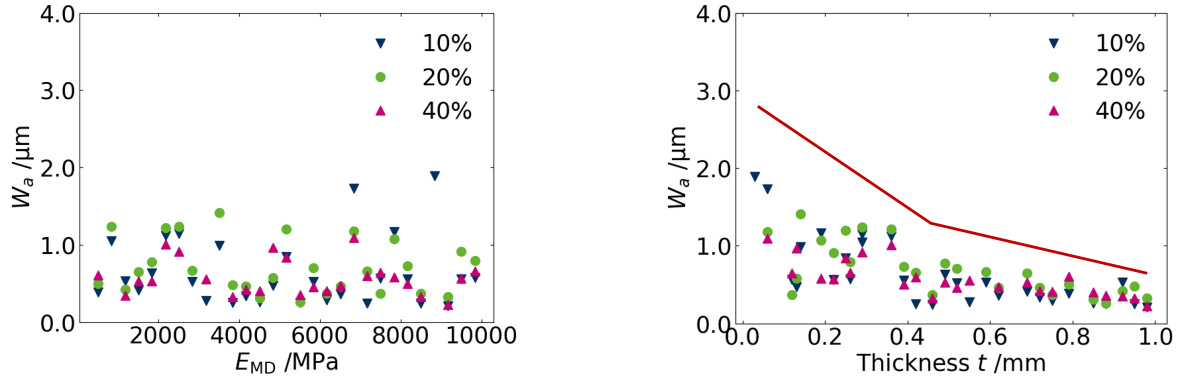

(a) Influence of E_{MD} (b) Influence of layer thickness t

Fig. 11: Relationship between the properties of the intermediate layer and the waviness W_a

The results from the simulations are shown Fig.11 (a) and (b). An unexpected finding is that there is no discernible correlation between stiffness and waviness, see Fig.11 (a). A possible explanation for this might be that the intermediate layer is so thin that its stiffness is negligible for the entire structure. As shown in Fig.11 (b), surface waviness W_a decreases with increasing thickness, significantly in the range of 0 to 0.4 mm.

The results of the simulations show that the layer thickness is the decisive factor for the waviness formation and the stiffness of this layer is of less importance.

4 Conclusions and Outlook

In this work, a numerical model was developed to represent the pressing process to analyze the causes of the unevenness of the exterior surface of sandwich panels with sinusoidal cores. While the height profile of the decorative layer could be extracted

directly from the simulation results, the height profile of the manufactured parts was measured with the Keyence VR 3200 Profilometer. A Gaussian filter was applied to the profiles to analyze them exclusively in the wavelength range between 0.8 and 8 mm. The comparison of experimental and simulation results using various random initial phase shifts indicate a reasonable agreement. The validated model was used to investigate the relationship between the properties of the intermediate/bottom layer and the surface waviness of the pressed panel using the DoE approach. Finally, a significant effect of the layer thickness was found, while the stiffness showed almost no influence.

A natural progression of this work is the analysis of correlations between other sandwich panel parameters and the waviness, such as the characteristics of the corrugated core. Furthermore, the adhesive materials for bonding the layers were not considered in the model. The geometrical differences and the effects of the adhesives need to be further investigated since no experimental data are available in the present study.

Acknowledgements The research project was carried out in the framework of the industrial collective research programme (IGF no. 20956 N). It was supported by the Federal Ministry for Economic Affairs and Energy (BMWi) through the AiF (German Federation of Industrial Research Associations eV) based on a decision taken by the German Bundestag. Furthermore, the authors gratefully acknowledge the GWK support for funding this project by providing computing time through the Center for Information Services and HPC (ZIH) at TU Dresden.

References

[1] R., Paul. and W., Klusmeier, Structhan®–A Composite with a Future (Status Report, Bayer AG, Leverkusen, Germany, 1997).
[2] Y., Wei., Dimensional stability of paper-based sandwich panels during the quasi-static pressing process, ECCM20 (2022).
[3] H, Kang, Assessment of Paint Appearance Quality in the Automotive Industry, Doctoral Thesis (Brunel University, England, 2000).
[4] W, Reuter., Hochleistungs-Faser-Kunststoff-Verbunde mit Class-A-Oberflächenqualität für den Einsatz in der Fahrzeugaußenhaut Doctoral Thesis (Kaiserlautern University, Germany, 2001).
[5] M., Britzke. Verfahren zur automatisierten Fertigung rahmenloser Sandwichplatten mit Papierwabenkern (2009).
[6] K., Persson., Material model for paper: experimental and theoretical aspects, M.Sc. diploma thesis (Lund University, Sweden, 1991).
[7] RW., Mann, GA., Baum, CC., Habeger Jr, Determination of all nine orthotropic elastic constants for machine-made paper, Tappi J;63:163-6 (1980).
[8] L., Beldie, Mechanics of paperboard packages–performance at short term static loading, M.Sc. thesis (Lund University, Sweden, 2001).
[9] T.M., Nordstrand, Parametric study of the post-buckling strength of structural core sandwich panels, Composite Struct 30, p.441-451 (1995).
[10] ISO 13565: Surface texture: Profile method; Surfaces having stratified functional properties (1997).
[11] M., Smith., ABAQUS/Standard User's Manual (Version 2020).
[12] M.,Britze, Verfahren zur automatisierten Fertigung rahmenloser Sandwichplatten mit Papierwabenkern, Lightweight Des **2**, p.55-62 (2009).